

Self-Organization in the Two-Dimensional Kelvin-Helmholtz Instability at the Magnetopause

MIURA Akira

Department of Earth and Planetary Physics, University of Tokyo, Tokyo 113-0033, Japan

(Received: 8 December 1998 / Accepted: 17 February 1999)

Abstract

A two-dimensional (2-D) magnetohydrodynamic (MHD) simulation of the Kelvin-Helmholtz (K-H) instability is performed in the plane transverse to the magnetic field for a random initial velocity perturbation. The relative constancy of the total kinetic energy and a rapid decay of the enstrophy by the selective dissipation with the numerical viscosity indicate that the successive pairings of vortices occurring in the nonlinear stage of the K-H instability is a self-organization process. The spectral distributions of the integrated kinetic energy, the enstrophy, and the integrated magnetic energy show power law distributions at the medium subrange of the wavenumber in the well developed nonlinear stage.

Keywords:

self-organization, Kelvin-Helmholtz instability, sheared plasma flow, MHD, magnetopause

1. Introduction

The shear in the flow velocity is a ubiquitous feature in space and astrophysical plasmas and it is susceptible to the K-H instability. The importance of the velocity shear in the fusion plasma confinement has also been recognized recently. The K-H instability occurring at the terrestrial magnetopause is a prototype example of the K-H instability occurring in the MHD sheared flows [1]. The nonlinear evolution of the K-H instability is responsible for the transport of momentum and energy across the velocity shear layer [1]. The pairing of vortices occurring in the nonlinear stage of the instability is a well-known nonlinear effect [1]. It has been shown by a 2-D MHD simulation starting from a coherent initial seed perturbation that the successive pairings of vortices occurring in the nonlinear stage of the K-H instability is a self-organization process [2]. The purpose of this brief report is to show that the self-organization in the K-H instability, i.e., the successive pairings of vortices, also arises for a random initial

velocity perturbation and the qualitative feature of the self-organization in the 2-D K-H instability is rather insensitive to the form of the initial seed perturbation.

2. Simulation Model

A 2-D MHD simulation of the K-H instability is performed for an initial velocity profile of $v_{0y}(x) = (V_0/2) [1 - \tanh(x/a)]$ and for a convective fast mode Mach number of 0.35 [1-2]. The initial uniform magnetic field is perpendicular to the simulation plane (x - y plane). Time t is normalized by $2a/V_0$, where $2a$ is the initial thickness of the velocity shear layer and V_0 is the total jump of the flow velocity across the velocity shear layer. The length of the periodic simulation box in the y -direction is equal to 8 times as long as the wavelength of the linearly fastest growing mode ($\lambda_{FGM} = 15.7a$) [3]. In Miura [2] a coherent perturbation, which was a sum of the linearly fastest growing mode and its subharmonics, was given as an initial seed perturbation

with the peak amplitude of v_x equal to $0.005V_0$ and the temporal evolution of the instability was investigated. In order to see the dependence of the self-organization on the initial perturbation a random velocity perturbation with its peak amplitude of v_x equal to $0.00005V_0$ is given as an initial seed perturbation in the present run. A two-step Lax-Wendroff scheme with an artificial viscosity is used in the present simulation and the number of grid points is equal to 400×400 .

3. Simulation Results

Figure 1 shows temporal evolutions of the total energy (dotted curve), total internal energy (dashed curve), total magnetic energy (dot-dash curve), and the total kinetic energy (solid curve) integrated in the whole simulation region. Each total energy is normalized by $0.0628a^2p_0$, where p_0 is the initial uniform pressure. It is obvious from this figure that the total kinetic energy remains almost constant during the simulation run in the present 2-D MHD transverse configuration.

Figure 2 shows temporal evolutions of the total square vorticity (enstrophy) integrated in the whole simulation region (solid curve), the contribution to the change of the total square vorticity due to the compressibility (dotted curve) and the baroclinic contribution to the change of the enstrophy (dashed curve), which are normalized by V_0^2 . It is obviously seen in this figure that the enstrophy decreases rapidly with time with a small oscillating component, which is due to the compressibility. It is also seen in this figure that the baroclinic term is negligible. Since the time change of the enstrophy is equal to the sum of the compressible

term, the baroclinic term, and the viscous term [1-2], we conclude that the rapid decay in the enstrophy shown in Figure 2 must be due to the viscous dissipation. Notice that although the present simulation is done for the ideal MHD without any explicit physical viscosity, small implicit numerical and artificial viscosities are included to prevent spurious mesh oscillations. Therefore, the enstrophy, which is the invariant in the 2-D, inviscid, and incompressible case, decreases with time due to the selective dissipation [4] by the numerical viscosity. The relative constancy of the total kinetic energy shown in Figure 1 and the selective decay of the enstrophy shown in Figure 2 are similar to the results obtained for a coherent initial seed perturbation [2] and indicate that the evolution of the K-H instability in the present 2-D MHD transverse configuration is a self-organization process [5].

Figure 3 shows the spectral amplitudes of the kinetic energy integrated across x versus the wavenumber in the y direction at $T = 0$ (a) and $T = 600$ (b), where $T = tV_0/(2a)$, the spectral amplitudes of the enstrophy versus the wavenumber at $T = 0$ (c) and $T = 600$ (d), and the spectral amplitudes of the magnetic energy integrated across x versus the wavenumber at $T = 0$ (e) and $T = 600$ (f). The spectral amplitudes of the integrated kinetic energy are normalized by $2ap_0$. The spectral amplitudes of the enstrophy are normalized by $(V_0/2a)^2$. The spectral amplitudes of the integrated magnetic energy are normalized by $a\mu_0^{-1}B_0^2$, where B_0 is the initial uniform magnetic field strength. In this figure k_{min} is the wavenumber equal to $k_{FGM}/8$, where k_{FGM} is the wavenumber in the y direction of the linearly fastest

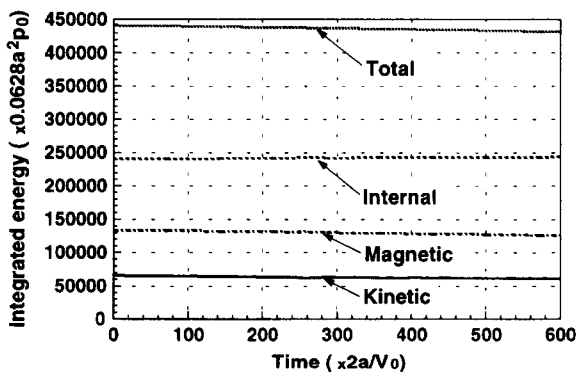


Fig. 1 Temporal evolutions of the total energy, total internal energy, total magnetic energy, and the total kinetic energy in the whole simulation region.

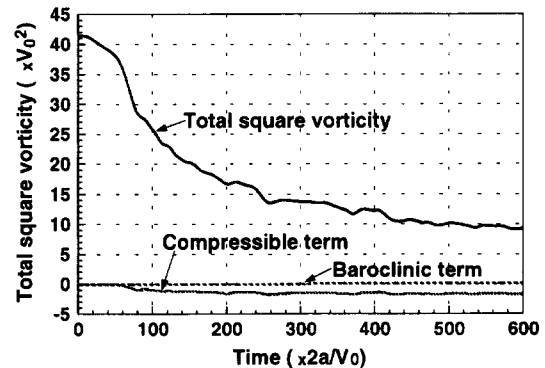


Fig. 2 Temporal evolutions of the total square vorticity (enstrophy), the contribution of the compressible term to the change of the enstrophy, and the contribution of the baroclinic term to the change of the enstrophy.

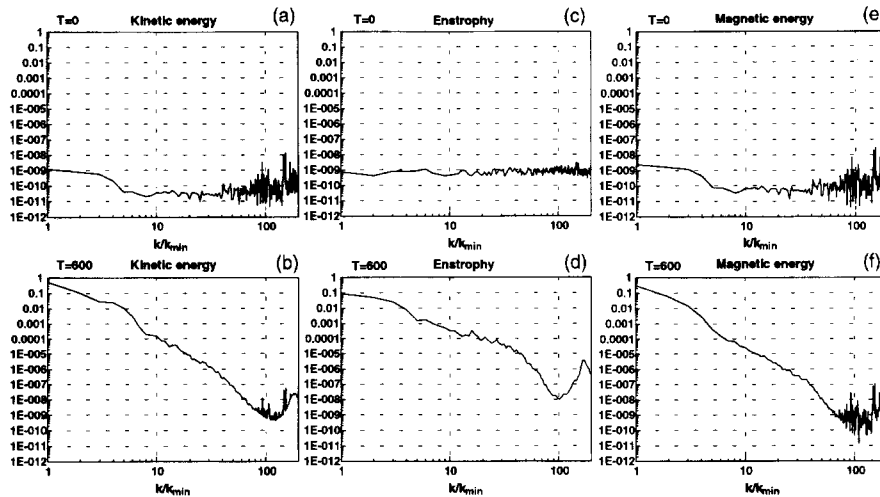


Fig. 3 The spectral amplitudes of the total kinetic energy versus the wavenumber at $T = 0$ (a) and $T = 600$ (b), the enstrophy at $T = 0$ (c) and $T = 600$ (d), and the total magnetic energy at $T = 0$ (e) and $T = 600$ (f).

growing mode. At $T = 0$, a random incompressible velocity perturbation with a small amplitude was added to the background flow velocity. Figures 3(a) and 3(c) show that the spectral distributions of the integrated kinetic energy and enstrophy at $T = 0$ are almost flat (white noise). However, at $T = 600$, the spectral distributions of the integrated kinetic energy, the enstrophy, and the integrated magnetic energy become almost continuous and are well represented by power law distributions at $k/k_{\min} < 90$. Irregular noise components at large k values ($k/k_{\min} > 90$) at $T = 600$ appeared because of the artificial viscosity added to the system. The spectral peaks at $k = k_{\min}$ at $T = 600$ of the integrated kinetic energy, the enstrophy, and the integrated magnetic energy occurred because of the inverse cascade. The power law exponents of the integrated kinetic energy, the enstrophy, and the integrated magnetic energy at medium subrange of the wavenumber from $k/k_{\min} = 10$ to 50 at $T = 600$ are equal to -4.61 , -2.58 , and -4.60 , respectively. Since the enstrophy is an integral of the square of curl of \mathbf{v} , the observed fact that the power law exponent of the enstrophy is nearly equal to the power law exponent of the total kinetic energy plus 2 is reasonable. Notice that the selective dissipation of the enstrophy and the relative constancy of the total kinetic energy are caused by the large difference of the power law exponents between the spectra of the integrated kinetic energy and the enstrophy.

Figures 4(a) and (c) show contours of vorticity at $T = 70$ and $T = 600$. At $T = 70$ eight vortices are observed

as predicted by the linear theory [3], but as a consequence of successive pairings of vortices, a large isolated vortex is formed inside the simulation region at $T = 600$. Figures 4(b) and (d) show electric current vectors at $T = 70$ and $T = 600$. It is seen in these panels that an eddy current is associated with each flow vortex. These eddy currents appear because of the compressibility, i.e., the eddy current is equal to curl of the z component of the magnetic field perturbation (fast magnetosonic component of the magnetic field). These currents are mainly carried by the inertia current [1-2].

4. Conclusion

By a 2-D MHD simulation of the K-H instability starting from a random velocity perturbation it has been established that the successive pairings of vortices occurring in the nonlinear stage of the instability is a self-organization process and the qualitative feature of the self-organization process is rather insensitive to the form of the initial seed perturbation. The present result, if applied to the spatial growth of the instability along the magnetopause, suggests that small-scale vortices excited at the dayside magnetopause by the instability evolve into global scale vortices in the tail of the magnetosphere by the successive pairings of vortices. Therefore, the self-organization process is responsible for the creation of a large scale order (vortex) in the tail of the magnetosphere.

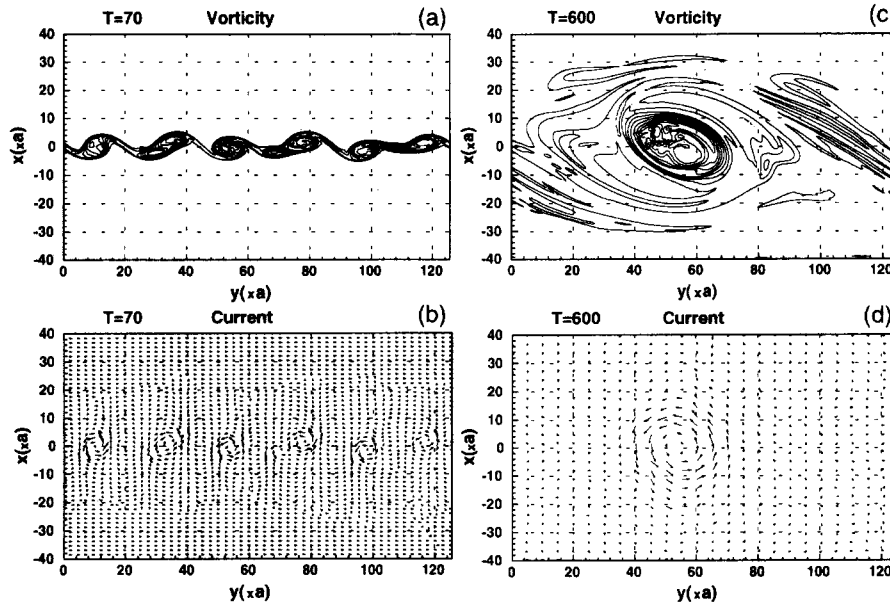


Fig. 4 (a) Contours of the vorticity at $T = 70$. (b) Electric current vectors at $T = 70$. (c) Contours of the vorticity at $T = 600$. (d) Electric current vectors at $T = 600$.

Acknowledgements

This work has been supported by Grants-in-aid for Scientific Research 09640529 and, in part, by RASC of Kyoto university, ISAS and CRL as a joint research project. The computation for this work was performed at the computer center of the University of Tokyo.

References

- [1] A. Miura, Phys. Plasmas **4**, 2871 (1997).
- [2] A. Miura, J. Geophys. Res. **104**, 395 (1999).
- [3] A. Miura and P.L. Pritchett, J. Geophys. Res. **87**, 7431 (1982).
- [4] D. Montgomery, L. Turner and G. Vahala, Phys. Fluids, **21**, 757 (1978).
- [5] A. Hasegawa, Adv. Phys. **34**, 1 (1985).